4-1992

HR 266=ADS 784: an Early Type Spectroscopic, Speckle Astrometric Multiple System

Warren A. Cole
Vanderbilt University

Francis C. Fekel
Vanderbilt University

William I. Hartkopf
Georgia State University

Harold A. McAlister
Georgia State University

Jocelyn Tomkin
University of Texas at Austin

HR 266 = ADS 784: AN EARLY TYPE SPECTROSCOPIC, SPECKLE ASTROMETRIC MULTIPLE SYSTEM

WARREN A. COLE AND FRANCIS C. FEKEL[1]
Department of Physics and Astronomy, Dyer Observatory, Vanderbilt University, Nashville, Tennessee 37235

WILLIAM I. HARTKOPF[1] AND HAROLD A. MCALISTER[1]
Center for High Angular Resolution Astronomy, Georgia State University, Atlanta, Georgia 30303

JOCELYN TOMKIN
Department of Astronomy, University of Texas, Austin, Texas 78712
Received 15 October 1991; revised 27 November 1991

ABSTRACT

The star HR 266 is thought to be a quadruple system of "Hierarchy 3." The short-period binary, with components *Ba* and *Bb*, has a period of 4.241 148 ± 0.000 008 d. The close pair orbits an unseen companion, *Bc*, with a period of 1769 ± 10 d. This companion has been detected independently by spectroscopic and speckle observations. The long-period or visual orbit of this triple and component *A* has a period of 83.10 ± 0.20 yr. The speckle detection of *Bc* as a submotion in the long-period orbit represents the first detection of a "speckle astrometric" system. Two possible models of the system's components are considered. The preferred model assumes that *Bb* is an A1 V star with a mass of $2.25\mathcal{M}_\odot$. Then, *Ba* has a mass of $3.4 \pm 0.8\,\mathcal{M}_\odot$ and a spectral type of B9 IV. Component *A* is a B7 IV star with an assumed mass of $5\mathcal{M}_\odot$. From the mass of *Bb*, the inclination of the short-period orbit is 54° ± 5°. Since the long-period orbit has an inclination of 54°.9 ± 1°.1 and the intermediate-period orbit appears to have an inclination of roughly 55° ± 5°, all three orbits may be coplanar. Component *Bc* has a minimum mass of $2.4\mathcal{M}_\odot$ that increases to $2.8\mathcal{M}_\odot$ if the intermediate-period orbit is coplanar. Such a value suggests that the *Bc* component's absorption features might be seen in our spectra, but this is not the case. Either *Bc* is a rapidly rotating single star, similar to *A*, or *Bc* is actually a pair of late type, lower-mass stars. The estimated distance to the system is 184 pc.

1. INTRODUCTION

HR 266 [HD 5408 = Bu 1099 = ADS 784, $\alpha(2000) = 0^h56^m\,47^s$, $\delta(2000) = +60°\,22'$, $V = 5.57$, spectral type = B9 Vn or B9 IVn] is a multiple-star system that has been studied for about 100 yr. In 1889, Burnham (1906) found the star to be a close visual double. The most recent published visual orbit for this pair has a period of 83.4 yr (Heintz 1978a).

Velocity variations of nearly 50 km s^{-1} were detected by Plaskett *et al.* (1922), while Frost *et al.* (1926) found a range of 90 km s^{-1}. Plaskett *et al.* (1922) noted that the absorption lines varied in character from plate to plate, being quite sharp on one photographic plate but rather diffuse on others. More recently, Palmer *et al.* (1968) also found the velocity to be variable and determined a very large value of 255 km s^{-1} for $v \sin i$. Abt *et al.* (1980) and Stickland & Weatherby (1984) have obtained a few additional velocities of HR 266.

Morgan (1931) reported the presence of manganese lines in the spectrum of HR 266 and the star is now classified as an HgMn star. The presence of such abundance anomalies, presumably as a result of diffusion, implies narrow lines and slow rotation in apparent conflict with the large $v \sin i$ of Palmer *et al.* (1968).

These various and somewhat conflicting spectroscopic observations led Fekel (1979) to begin an extensive high-dispersion spectroscopic investigation of the system with photographic plates and Reticon spectrograms. From these observations he detected lines of three components (Fig. 1). He identified component *A* as a B7 V broad-lined star and found its visual companion, component *B*, to be a short-period double-lined binary. *Ba* and *Bb* are narrow lined and were classified as B9 V HgMn for *Ba* and A1 V for *Bb*.

Fekel (1979) determined two orbital solutions for the short-period binary, one from data obtained in 1975 and 1976, which has been listed in the spectroscopic binary catalog of Batten *et al.* (1989), and the other from data obtained in 1977 and 1978. The orbital elements of the two sets were significantly different. The center of mass, or γ velocities, differed by more than 13 km s^{-1} and the other elements differed by more than their mean errors. These differences could not be due to the motion in the visual orbit, since this would not change so drastically in such a short time. Fekel (1979) concluded that *Ba* and *Bb* must be in an orbit with an unseen component, which will be called *Bc*, and that this triple and component *A* make up the visual binary system. According to Evans' (1968) classification, this multiple system is of Hierarchy 3. A mobile diagram (Evans 1968) of the system (Fig. 2) shows the relationship of these components and some of their properties.

A note on terminology is perhaps in order here. The advent of techniques such as speckle interferometry, coupled with continuing improvements in radial-velocity measurements, has increasingly blurred the distinction between traditional binary star classifications such as "spectroscopic," "visual," "astrometric," and the like. To avoid confusion in discussing the various hierarchical components in the HR 266 system, we will refer to the pairs as follows: the 83 yr period visual or "*AB*" pair is referred to as the "long-period"

[1] Visiting Astronomer, Kitt Peak National Observatory, National Optical Astronomy Observatories, operated by the Association of Universities for Research, Inc., under contract with the National Science Foundation.

 0004-6256/92/041357-12$00.90

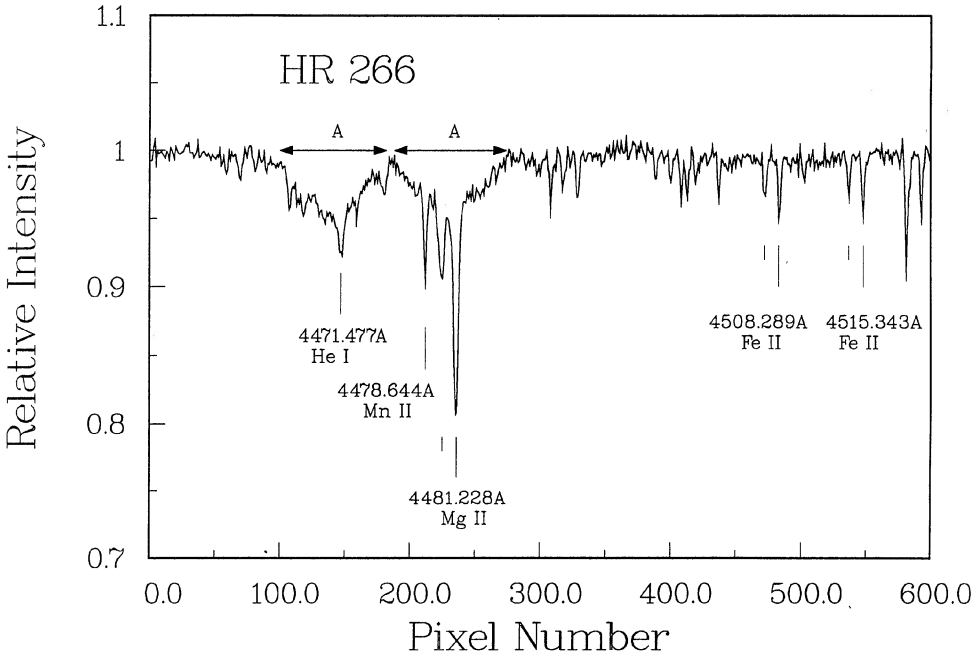

FIG. 1. A portion of a TI CCD spectrum of HR 266 showing the lines of *A* (arrows), *Ba* (long tick marks), and *Bb* (short tick marks).

pair; the 4.2 d spectroscopic or "*Bab*" pair is the "short-period" pair, and the 1769 d astrometric or "*Bab,c*" pair is the "intermediate" pair. Orbital elements will be subscripted with the letters *L*, *S*, and *I* to aid in this distinction.

2. SPECTROSCOPIC OBSERVATIONS AND DATA REDUCTION

A total of 95 spectroscopic observations have been obtained from 1975 to 1990 with a variety of telescope and detector combinations (Table 1). Fifty-nine observations were obtained with II*a*O photographic plates from 1975 to 1980 at either McDonald Observatory or the Dominion Astrophysical Observatory (DAO). The rest were acquired with solid-state detectors between 1978 and 1990. Sixteen observations were obtained at McDonald Observatory with a Reticon RL 1024B silicon photo diode array (Vogt *et al.* 1978), while 20 observations were made at Kitt Peak National Observatory (KPNO) with a TI CCD detector.

The McDonald and DAO plates of HR 266 were measured either with a Grant measuring machine at Johnson Space Center, Houston, Texas, or with the Arcturus measuring machine at the DAO, Victoria, British Columbia. The lines of component *A* were too broad to be measured accurately. Between 10 and 20 lines were measured for *Ba*, while usually only two or three lines (Ca II *K* 3933 Å, Mg II 4481 Å, and Fe II, Ti II 4549 Å) were measured for *Bb*. A correction of -0.5 km s^{-1} has been added to the McDonald plate velocities to place them on the velocity system of Scarfe *et al.* (1990).

There are no International Astronomical Union (IAU) radial-velocity standard stars with spectral types earlier than F5 (Pearce 1957). Thus, we call the stars used to determine the velocities of HR 266 reference stars. The properties of the reference stars used for the Reticon and CCD observations are listed in Table 2.

The reference star 68 Tau was suspected of having a variable radial velocity. From four observations between 1905 and 1910, Campbell & Moore (1928) found a velocity of 36.3 km s^{-1}. Stickland (1980) found an average velocity of 35.8 km s^{-1} from eight plates obtained between late 1972 and early 1973. However, Fekel (1985) determined a velocity of 39.5 km s^{-1} from three more recent observations. To see whether its velocity varied during the time of our observations, 68 Tau was treated as a program star, and its velocity was determined relative to the radial-velocity standard stars 10 Tau and ι Psc (Table 2). Radial velocities for 68 Tau over a 10 yr period of observation from 1979 to 1989 were determined with the method described by Fekel *et al.* (1978). The three velocities measured by Fekel are also included in this study. The results are listed in Table 3 along with the appropriate source codes. No significant systematic radial-velocity increase or decrease is evident over this time period. It is, therefore, assumed that 68 Tau has a constant radial velocity of 39.0 $\pm$ 0.2 km s^{-1}. If 68 Tau is variable, it is on a much longer timescale than that of our observations.

The radial velocities of *Ba* and *Bb* from the spectra ob-

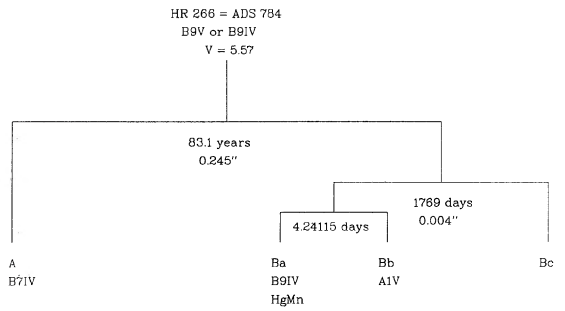

FIG. 2. Mobile diagram of HR 266 and some of its properties.

TABLE 1. Telescope-detector combinations.

Observatory	Telescope	Detector	Dispersion (Å mm^{-1})	Resolution (Å)	Wavelength region (Å)	Source code
McDonald	2.1 m	IIaO plate	8.5	0.17	3800–4600	MP
DAO	1.2 m	IIaO plate	6.5	0.13	3800–4600	DAOP
McDonald	2.1 m	IIaO plate	3.3	0.07	3750–4325	MPB1
McDonald	2.1 m	IIaO plate	3.3	0.07	4070–4600	MPB2
McDonald	2.7 m	Reticon	4.4	0.36	6300–6400	MRR
McDonald	2.7 m	Reticon	4.4	0.33	4450–4550	MRB
KPNO	Coudé feed	IIaO plate	8.9	0.18	3800–4600	KP
KPNO	Coudé feed	TI CCD	7.6	0.25	6325–6415	KTR1
KPNO	Coudé feed	TI CCD	3.8	0.25	4473–4519	KTB1
KPNO	Coudé feed	TI CCD	7.0	0.18	6385–6470	KTR2
KPNO	Coudé feed	TI CCD	7.0	0.21	4460–4545	KTB2

tained with the Reticon and CCD detectors were determined with the method described by Fekel *et al.* (1978). Most of these cover a wavelength range of about 100 Å or less centered at about 4500 Å. This process of measuring radial velocities was performed four times for each spectrum, twice for *Ba* and twice for *Bb*. Because the Mg II line at 4481 Å is so much stronger than any other measurable line in the observed wavelength region, its velocity was measured alone. A second velocity was determined from the composite line profile of several weak absorption lines of Fe II and Ti II. These two radial-velocity values for each of the stars of the close binary usually differed by less than 0.7 km s^{-1}, and so, a simple average was determined. In three spectra, the 4481 Å line of *Bb* was blended with the 4478 Å Mn II feature of *Ba*, so the velocity was determined from the Fe II and Ti II lines only. Finally, in two cases, the weak lines were difficult to distinguish from the continuum and the suspect velocity from them was ignored. For spectra of the 6360 Å region, two Si II lines were measured. Only one velocity was found for each component in this case. The observed velocities for *Ba* and *Bb* are listed in Table 4.

3. SPECTROSCOPIC ORBITS

The heliocentric Julian Dates (HJD's) and the radial velocities of components *Ba* and *Bb* were used to calculate the short-period orbital elements of HR 266. The unseen *Bc* component, however, complicates this procedure. Motion in the intermediate-period orbit causes the center-of-mass velocity of the short-period pair, γ_S, to vary with time. To determine an approximate intermediate period, a plot of γ_S vs time was made. The value of γ_S for each observation was calculated with the equation

$$\gamma_s = [K_{Bb}/(K_{Ba} + K_{Bb})]V_{Ba} + [K_{Ba}/K_{Ba} + K_{Bb})]V_{Bb}$$

of Petrie & Batten (1970). The K's represent the semiamplitudes of *Ba* and *Bb*, and V_{Ba} and V_{Bb} are the radial velocities of the components for a given observation. In a first attempt to compute the γ's, we assumed the semiamplitude values of 88.2 and 121.5 km s^{-1} for *Ba* and *Bb* from Fekel's (1979) 1975 and 1976 observations. Although the variation of γ's appeared to be periodic, the scatter of the velocities was too great to determine an accurate period, presumably because the assumed semiamplitudes contain a component of motion in the intermediate orbit.

The γ velocity of the short-period pair changes least rapidly near its maximum and minimum values (Fig. 3). Since more observations were obtained near the minimum value, only observations with γ velocities between about -10 and -17 km s^{-1} were used to obtain improved short-period elements (the γ-minimum solution), including new values of the semiamplitudes of *Ba* and then *Bb*. A period-finding program (Bopp *et al.* 1970) was used to find the short period. With this period, preliminary orbital elements for *Ba*, the stronger-lined star, were computed with a program that uses a series of sines and cosines to determine a starting set of short-period elements (Wolfe *et al.* 1967). A set of improved short-period elements for *Ba* was calculated with a differential corrections program (Barker *et al.* 1967). With these elements as starting values, elements for *Bb* were computed with the differential corrections program.

TABLE 2. Reference and standard stars.

Standard star	Spectral type	V (km s^{-1})	Velocity source
10 Tau	F9 V	27.9	Scarfe *et al.* (1990)
68 Tau	A2 IV	39.0	Cole (this paper)
o Peg	A1 IV	8.7	Fekel (unpublished)
α Lyr	A0 V	-14.2	Campbell & Moore (1928)
ι Psc	F7 V	5.6	Scarfe *et al.* (1990)

TABLE 3. Radial velocities of 68 Tau (= HR 1389 = HD 27 962).

Date (UT)	HJD 2400 000 +	V (km s^{-1})	Standard star	Lines measured	Source code
10/31/79	44 177.841	39.4	10 Tau	4	MRB
10/31/79	44 177.958	38.1	10 Tau	3	MRR
11/01/79	44 178.792	39.0	10 Tau	5	MRB
08/29/84	45 941.990	38.9	ι Psc	5	KTR1
09/28/84	45 971.957	39.9	ι Psc	3	KTR1
09/30/84	45 973.941	37.2	10 Tau	4	KTR1
11/19/85	46 388.904	39.0	10 Tau	5	KTR1
11/21/85	46 390.722	39.2	ι Psc	5	KTR1
11/23/85	46 392.997	40.1	10 Tau	5	KTR1
01/21/87	46 816.819	38.4	10 Tau	4	KTR1
03/13/87	46 867.632	38.9	10 Tau	4	KTR1
10/28/87	47 096.806	38.0	ι Psc	3	KTR1
03/24/88	47 244.612	39.3	10 Tau	3	KTR2
03/25/88	47 245.597	39.1	10 Tau	4	KTR2
03/28/88	47 248.591	39.7	10 Tau	6	KTR2
10/19/88	47 453.836	38.6	ι Psc	4	KTR2
10/21/88	47 455.998	38.9	10 Tau	4	KTR2
10/22/88	47 456.810	39.8	ι Psc	4	KTR2
10/23/88	47 458.000	38.3	10 Tau	4	KTR2
01/30/89	47 556.559	39.8	10 Tau	4	KTR2

TABLE 4. Velocity observations of HR 266.

Date (UT)	HJD 2400000+	V_{Ba} (km s^{-1})	V_{Bb} (km s^{-1})	Standard Star	Source Code
10/21/75	42706.914	-67.1	101.9	—	MP
10/23/75	42708.905	37.3	-58.3	—	MP
10/24/75	42709.812	92.7	—	—	MP
10/26/75	42711.832	-36.1	54.6	—	MP
10/27/75	42712.857	19.6	-37.4	—	MP
12/16/75	42762.761	-36.5	51.9	—	MP
12/17/75	42763.569	5.0	—	—	MP
12/18/75	42764.670	82.8	—	—	MP
01/16/76	42793.686	31.1	-53.4	—	MP
03/14/76	42851.589	-47.8	66.3	—	MP
03/15/76	42852.576	-2.4	—	—	MP
03/16/76	42853.578	67.3	—	—	MP
03/17/76	42854.572	-37.4	35.6	—	MP
03/19/76	42856.582	-9.8	—	—	MP
06/18/76	42947.966	-59.7	65.7	—	DAOP
06/27/76	42956.975	-84.0	96.9	—	DAOP
07/12/76	42971.988	38.2	-90.4	—	DAOP
08/08/76	42998.965	-70.9	90.2	—	MP
08/09/76	42999.965	-58.8	62.9	—	MP
08/11/76	43001.973	60.3	-112.8	—	MP
08/12/76	43002.970	-30.6	26.6	—	MP
09/15/76	43037.024	-59.9	59.4	—	DAOP
10/09/76	43060.853	24.2	-65.6	—	MP
10/10/76	43061.903	75.7	—	—	MP
10/11/76	43062.876	-81.7	93.1	—	MP
10/12/76	43063.922	-42.4	38.3	—	MP
10/14/76	43065.707	69.2	-124.2	—	MP
11/02/76	43084.888	-56.6	51.2	—	MP
11/04/76	43086.741	54.6	-111.6	—	MP
11/05/76	43087.801	-37.5	22.8	—	DAOP
11/29/76	43111.608	11.2	—	—	DAOP
12/08/76	43120.805	61.5	-127.2	—	MP
12/10/76	43122.745	-70.3	78.9	—	MP
01/08/77	43151.557	-64.3	66.3	—	MP
01/11/77	43154.675	59.6	-122.5	—	MP
01/13/77	43156.638	-75.1	74.7	—	MP
04/20/77	43253.694	-91.8	193.6	—	DAOP
05/06/77	43269.957	23.7	-72.2	—	MP
05/07/77	43270.976	-82.1	89.3	—	MP
07/10/77	43334.970	-68.9	—	—	MP
07/11/77	43335.971	-15.5	—	—	MP
09/03/77	43389.726	-81.7	92.5	—	MP
09/03/77	43389.955	-74.1	77.3	—	MP
09/04/77	43390.936	-24.0	—	—	MP
09/06/77	43392.691	72.9	—	—	MP
10/31/77	43447.639	76.7	-156.6	—	MP

TABLE 4. (continued)

Date (UT)	HJD 2400000+	V_{Ba} (km s^{-1})	V_{Bb} (km s^{-1})	Standard Star	Source Code
11/01/77	43448.671	-87.8	87.6	—	MPB1
11/01/77	43448.692	-90.0	181.3	—	MP
11/02/77	43449.579	-63.9	—	—	MP
11/03/77	43450.773	0.2	—	—	MP
11/04/77	43451.759	69.1	—	—	MPB1
11/04/77	43451.808	71.6	—	—	MPB2
02/01/78	43540.636	54.2	-132.9	—	MP
02/02/78	43541.569	-35.9	—	—	MP
02/03/78	43542.655	-76.8	—	—	MPB1
08/20/78	43740.896	-34.5	17.3	68 Tau	MRR
08/21/78	43742.000	-70.1	71.6	68 Tau	MRR
08/22/78	43742.863	-28.8	13.7	68 Tau	MRR
08/24/78	43744.872	44.0	-101.9	o Peg	MRB
08/25/78	43745.858	-83.4	88.8	68 Tau	MRB
12/18/78	43860.596	-71.1	89.8	—	MP
06/18/79	44042.968	-61.0	94.0	o Peg	MRB
10/31/79	44177.841	-40.9	68.4	68 Tau	MRB
11/01/79	44178.778	-55.7	93.3	68 Tau	MRB
11/02/79	44179.870	0.4	—	68 Tau	MRB
11/03/79	44180.895	64.0	-93.6	68 Tau	MRB
08/21/80	44472.959	17.7	-34.8	68 Tau	MRB
08/23/80	44474.957	-69.0	94.6	68 Tau	MRB
08/24/80	44475.818	-52.6	76.4	α Lyr	MRB
08/26/80	44477.864	65.7	—	—	KP
08/27/80	44478.790	1.1	—	—	KP
08/29/80	44480.874	-14.5	—	—	KP
01/22/81	44636.569	81.6	-136.6	68 Tau	MRB
08/17/81	44833.821	34.7	-83.3	α Lyr	MRB
10/18/81	44895.775	-59.1	62.3	68 Tau	MRB
09/17/83	45594.843	-85.0	99.0	o Peg	KTB1
09/18/83	45595.921	-42.2	32.4	o Peg	KTB1
09/19/83	45596.903	12.1	-53.2	68 Tau	KTB1
01/18/84	45717.646	-74.9	101.6	68 Tau	KTB1
01/19/84	45718.638	-48.3	64.2	68 Tau	KTB1
09/28/84	45971.828	-34.2	58.2	o Peg	KTB1
11/19/85	46388.699	-54.1	65.9	o Peg	KTB1
11/21/85	46390.795	75.1	-127.8	68 Tau	KTB1
11/23/85	46392.792	-68.9	72.7	68 Tau	KTB1
10/15/86	46718.912	-84.2	94.6	68 Tau	KTB1
10/17/86	46720.828	12.4	-52.9	68 Tau	KTB1
10/22/88	47456.846	-81.1	97.3	68 Tau	KTB2
10/23/88	47457.828	-37.1	31.0	68 Tau	KTB2
10/24/88	47458.850	22.9	-58.1	68 Tau	KTB2
01/30/89	47556.666	46.6	-83.0	68 Tau	KTB2
10/11/89	47810.850	31.1	-46.3	68 Tau	KTB2
10/13/89	47812.871	-73.1	111.7	68 Tau	KTB2
10/14/89	47813.898	-35.9	58.3	68 Tau	KTB2
10/15/89	47814.887	17.6	-29.2	68 Tau	KTB2
01/26/90	47917.762	89.1	—	68 Tau	KTB2

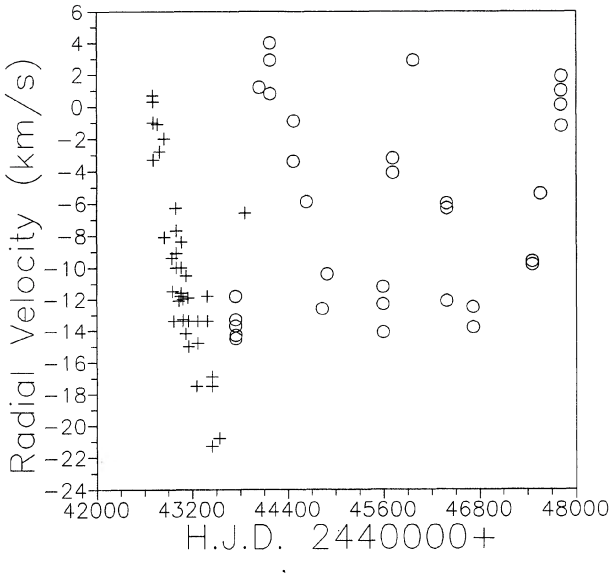

FIG. 3. Center-of-mass velocity plotted vs heliocentric Julian Date for the short-period binary *Ba-Bb*. The crosses represent photographic plate measurements, while the circles indicate Reticon or CCD observations.

TABLE 5. Final orbital elements for HR 266.

	Short period	Intermediate period	Long period
P (d)	4.241146 ± 0.000008	1769 ± 10	30351 ± 72
P (yr)		4.84 ± 0.03*	83.10 ± 0.20
T (HJD)	2445971.576 ± 0.007	2445740 ± 38	2434126 ± 34
T (BY)	1984.74175 ± 0.00002	1984.11 ± 0.10*	1952.31 ± 0.09
K_{Ba}	82.8 ± 0.3 km s^{-1}		
K_{Bb}	123.7 ± 1.0 km s^{-1}		
K_{Bab}		10.5 ± 0.3 km s^{-1}	
γ	Variable	-8.7 ± 0.2 km s^{-1}	
e	0.415 ± 0.003	0.23 ± 0.03*	0.241 ± 0.002
ω_{Ba}	$72\overset{\circ}{.}8 \pm 0\overset{\circ}{.}6$		
ω_{Bb}	$253° \pm 1°$		
ω		$290° \pm 9°$*	$333\overset{\circ}{.}19 \pm 0\overset{\circ}{.}33$
a''		$0''.004 \pm \sim 0''.002$	$0''.245 \pm 0''.002$
i		$55° \pm \sim 5°$	$54\overset{\circ}{.}9 \pm 1\overset{\circ}{.}1$
Ω		$185° \pm \sim 10°$	$175\overset{\circ}{.}01 \pm 0\overset{\circ}{.}33$
$a_{Ba} \sin i$	$4.39 \pm 0.03 \times 10^6$ km		
$a_{Bb} \sin i$	$6.57 \pm 0.06 \times 10^6$ km		
$a_{Bab} \sin i$		$2.56 \pm 0.11 \times 10^8$ km	
$M_{Ba} \sin^3 i$	$1.8 \pm 0.3\,\mathcal{M}_\odot$		
$M_{Bb} \sin^3 i$	$1.2 \pm 0.2\,\mathcal{M}_\odot$		
$f(m)$		$0.196\,\mathcal{M}_\odot$	

* Spectroscopic elements adopted in determination of visual elements.

The semiamplitudes of *Ba* and *Bb* from these γ-minimum solutions were used to compute new γ velocities for all the individual observations. The resulting plot of γ's vs time now appeared to show a period of about five years (e.g., Fig. 3). These calculated γ_S velocities were used with the previously mentioned computer programs to determine preliminary intermediate-period elements.

These intermediate-period elements and the short-period elements for *Ba* were used as starting values for a general least-squares program (Daniels 1966) that used differential corrections to solve simultaneously for both the short- and intermediate-period elements of *Ba*. Short- and intermediate-period orbital elements then were determined simultaneously for *Bb* with the same procedure. Although the lines of *Bb* are somewhat weaker than those of *Ba*, the values of the orbital elements for each component agreed to within their uncertainties.

Next, appropriate weighting of the data was considered. The differential-corrections program was run once with the photographic data of *Ba* only and again with the Reticon and CCD data of *Ba* only. As a result of these solutions, the Reticon and CCD data were given a weight of 1.0, while the photographic data were given a weight of 0.6. This procedure was repeated for the *Bb* component, and the weights found for the two data sets were the same as for the *Ba* component. Presumably, the CCD data have greater weight due to the higher signal-to-noise ratio of the spectra, but the photographic data have significant weight because numerous lines were measured.

The final intermediate- and short-period elements were calculated simultaneously with the differential-corrections program for *Ba* and then separately for *Bb*, with the data weighted appropriately. These elements are given in Table 5. The final intermediate-period value converged to 1769 ± 10 d with the appropriately weighted data of *Ba*. The intermediate-period elements were fixed at the final *Ba* element values when the differential-corrections program was executed for the *Bb* component, since the variation in amplitude is small for the intermediate-period radial-velocity curve and the individual velocity uncertainties are greater.

For plotting purposes each observed velocity (Table 4), which consists of the combined short-, intermediate-, and long-period variations, has been separated into a short-period velocity, V_S, and an intermediate-period velocity, V_I (Table 6). It has been assumed that the long-period velocity, V_L, did not change significantly during our years of observation. Each of the velocities, V_S and V_I, consists of its predicted velocity plus one half of the observed velocity residual. Those data for the radial-velocity curves for components *Ba* and *Bb* are shown in Fig. 4. Figure 5 shows the intermediate-period radial-velocity curve for *Ba*.

4. THE VISUAL ORBITS

In addition to having over a century of visual observations, ADS 784 has been observed regularly by CHARA and other speckle groups since 1977 (Worley 1990; McAlister & Hartkopf 1988; McAlister *et al.* 1990). New orbital elements for this long-period system have been determined with the "grid-search" method described by Hartkopf *et al.* (1989). Table 5 lists the newly determined elements, while Fig. 6 shows both that orbit and an earlier determination by Heintz (1978a). The new orbit revises the total mass 7.4% downward from the previous visual orbit.

A residual "wave" of roughly 5 yr period was noticed in the speckle data, and is apparent in the distribution of the speckle observations of Fig. 6, although those data were not of sufficient accuracy by themselves to derive orbital elements (Al-Shukri 1991). Shortly afterward, the CHARA and Dyer groups learned of each other's independent detections of the intermediate-period component and realized the usefulness of a joint solution. Thus, by a pleasant coincidence, each group was able to verify the other's discovery. This is believed to be the first multiple star component discovered both astrometrically and spectroscopically; it is also the first known example of a "speckle astrometric" binary.

TABLE 6. Radial velocities of HR 266B.

HJD 2400000+	Phase$_S$	V$_S$(Ba) (km s^{-1})	O-C (km s^{-1})	V$_S$(Bb) (km s^{-1})	O-C (km s^{-1})	Phase$_I$	V$_I$(Ba) (km s^{-1})	O-C (km s^{-1})
42706.914	0.241	-65.4	0.3	102.3	1.7	0.286	-1.7	0.3
42708.905	0.710	39.3	0.1	-58.4	2.3	0.287	-2.0	0.1
42709.812	0.924	93.4	1.5	—	—	0.287	-0.7	1.5
42711.832	0.400	-34.9	1.0	56.3	0.5	0.288	-1.2	1.0
42712.857	0.642	21.1	0.8	-33.3	-1.9	0.289	-1.4	0.8
42762.761	0.409	-33.6	0.6	54.3	1.1	0.317	-2.9	0.6
42763.569	0.599	8.9	-0.4	—	—	0.318	-3.9	-0.4
42764.670	0.859	85.5	0.9	—	—	0.318	-2.7	0.9
42793.686	0.700	5.9	-0.5	-52.7	3.6	0.335	-4.8	-0.5
42851.589	0.353	-43.8	1.8	71.3	0.8	0.367	-4.0	1.8
42852.576	0.586	4.6	-1.3	—	—	0.368	-7.0	-1.3
42853.578	0.822	73.5	-0.4	—	—	0.369	-6.2	-0.4
42854.572	0.056	-33.1	1.5	44.7	-3.3	0.369	-4.3	1.5
42856.582	0.530	-5.6	1.7	—	—	0.370	-4.2	1.7
42947.966	0.077	-51.3	-0.2	73.4	0.5	0.422	-8.4	-0.2
42956.975	0.201	-73.1	-2.5	106.2	-0.9	0.427	-10.9	-2.5
42971.988	0.741	47.7	-0.8	-78.4	-3.3	0.435	-9.5	-0.8
42998.965	0.102	-62.5	0.9	96.0	3.6	0.451	-8.4	1.0
42999.965	0.338	-49.0	-0.4	73.7	-1.4	0.451	-9.8	-0.4
43001.973	0.811	70.1	-0.4	-105.8	2.5	0.452	-9.8	-0.4
43002.970	0.046	-22.9	1.8	34.9	1.2	0.453	-7.7	1.8
43037.034	0.076	-49.9	0.3	70.7	-1.0	0.472	-10.0	0.3
43060.853	0.694	34.8	0.2	-54.4	-0.4	0.486	-10.6	0.2
43061.903	0.942	86.8	-0.3	—	—	0.486	-11.1	-0.3
43062.876	0.171	-71.7	0.9	106.6	-2.6	0.487	-10.0	0.9
43063.922	0.418	-31.8	0.4	49.6	-0.4	0.487	-10.6	0.4
43065.707	0.839	79.6	0.6	-116.9	3.7	0.488	-10.4	0.6
43084.888	0.361	-44.6	-0.7	65.2	-2.6	0.499	-12.1	-0.7
43086.741	0.798	66.2	-0.2	-101.2	1.0	0.500	-11.6	-0.2
43087.801	0.048	-26.4	0.3	35.6	-1.3	0.501	-11.1	0.3
43111.608	0.662	24.4	-1.2	—	—	0.514	-13.2	-1.2
43120.805	0.830	75.0	-1.4	-116.0	0.9	0.520	-13.5	-1.4
43122.745	0.288	-58.0	0.0	90.1	1.0	0.521	-12.3	0.0
43151.557	0.081	-52.4	1.0	78.0	1.1	0.537	-11.9	1.0
43154.675	0.816	72.3	0.2	-110.1	0.5	0.539	-12.7	0.2
43156.638	0.279	-60.8	-1.3	89.5	-1.9	0.540	-14.3	-1.3
43253.694	0.163	-74.8	-2.2	108.8	-0.3	0.595	-17.0	-2.2
43269.957	0.998	38.0	0.9	-55.1	-2.0	0.604	-14.3	0.9
43270.976	0.238	-66.5	-0.4	102.7	1.8	0.604	-15.6	-0.4
43334.970	0.327	-51.6	-1.0	—	—	0.641	-17.2	-1.0
43335.971	0.563	0.6	0.2	—	—	0.641	-16.1	0.2
43389.726	0.238	-65.4	0.7	105.2	4.3	0.672	-16.3	0.7
43389.955	0.292	-57.2	0.1	91.1	3.2	0.672	-16.9	0.1
43390.936	0.523	-8.0	1.1	—	—	0.672	-16.0	1.0
43392.691	0.937	89.4	0.5	—	—	0.673	-16.5	0.5
43447.639	0.893	93.1	1.4	-138.2	-0.7	0.704	-16.4	1.4

TABLE 6. (continued)

HJD 2400000+	Phase$_S$	V$_S$(Ba) (km s^{-1})	O-C (km s^{-1})	V$_S$(Bb) (km s^{-1})	O-C (km s^{-1})	Phase$_I$	V$_I$(Ba) (km s^{-1})	O-C (km s^{-1})
43448.671	0.136	-70.6	0.6	105.6	-0.3	0.705	-17.2	0.6
43448.692	0.141	-72.0	-0.3	103.0	-3.9	0.705	-18.0	-0.3
43449.579	0.350	-46.1	0.0	—	—	0.705	-17.8	0.0
43450.773	0.632	17.8	0.2	—	—	0.706	-17.6	0.2
43451.759	0.864	86.4	0.4	—	—	0.707	-17.3	0.4
43451.808	0.876	89.0	0.3	—	—	0.707	-17.4	0.3
43540.636	0.820	72.9	-0.4	-113.7	-0.9	0.757	-18.7	-0.4
43541.569	0.040	-17.6	0.1	—	—	0.757	-18.3	0.1
43542.655	0.296	-57.5	-1.0	—	—	0.758	-19.3	-1.0
43740.896	0.039	-17.2	-1.4	28.2	5.0	0.870	-17.3	-1.4
43742.000	0.299	-55.1	0.9	86.7	0.9	0.871	-15.0	0.9
43742.863	0.502	-13.3	0.4	25.3	4.3	0.871	-15.5	0.4
43744.872	0.976	61.4	-1.6	-87.5	1.5	0.872	-17.4	-1.6
43745.858	0.208	-68.7	1.1	105.3	-0.7	0.873	-14.7	1.1
43860.596	0.262	-61.3	1.1	98.0	2.7	0.938	-9.8	1.1
44042.968	0.263	-61.3	1.0	94.8	-0.2	0.041	0.3	0.9
44177.841	0.064	-42.3	-1.2	63.2	2.7	0.117	1.4	-1.2
44178.778	0.285	-58.4	0.1	90.1	0.7	0.118	2.7	0.1
44179.870	0.542	-3.4	1.2	—	—	0.118	3.8	1.2
44180.895	0.784	61.6	-0.2	-96.2	0.0	0.119	2.4	-0.2
44472.959	0.648	20.8	-1.1	-34.0	1.2	0.284	-3.1	-1.1
44474.957	0.119	-67.7	0.7	99.2	-2.5	0.285	-1.3	0.7
44475.818	0.322	-51.0	0.5	78.6	-0.2	0.286	-1.6	0.5
44477.864	0.805	68.1	-0.3	—	—	0.287	-2.4	-0.3
44478.790	0.023	3.4	-0.1	—	—	0.287	-2.3	-0.1
44480.874	0.514	-11.6	-0.6	—	—	0.288	-2.8	-0.6
44626.569	0.867	87.1	0.4	-131.5	0.8	0.371	-5.5	0.4
44833.821	0.734	46.0	-0.4	-72.9	0.5	0.488	-11.3	-0.4
44895.775	0.342	-47.3	0.5	73.7	0.9	0.523	-11.8	0.5
45594.843	0.172	-72.4	0.1	110.3	1.3	0.918	-12.6	0.1
45595.921	0.426	-30.1	0.4	45.4	-0.4	0.919	-12.2	0.4
45596.903	0.658	24.6	0.1	-40.4	-0.3	0.919	-12.4	0.1
45717.646	0.127	-69.6	0.3	106.0	1.2	0.988	-5.3	0.3
45718.638	0.361	-43.4	0.6	68.2	1.6	0.988	-5.0	0.6
45971.828	0.060	-37.2	0.4	57.4	-1.9	0.131	3.0	0.4
46388.699	0.352	-47.1	-1.3	70.4	1.3	0.367	-7.0	-1.3
46390.795	0.846	81.0	-0.1	-123.9	1.9	0.368	-5.9	-0.1
46392.792	0.317	-57.8	-5.2	79.0	-0.5	0.369	-11.0	-5.2
46718.912	0.211	-70.2	-0.6	106.4	1.6	0.554	-14.0	-0.6
46720.828	0.663	25.8	0.0	-41.2	1.8	0.555	-13.4	0.0
47456.846	0.205	-72.0	-1.7	105.1	-0.4	0.971	-9.2	-1.7
47457.828	0.437	-29.0	-0.8	39.8	-1.4	0.971	-8.1	-0.8
47458.850	0.677	30.1	0.2	-50.4	-0.4	0.972	-7.2	0.2
47556.666	0.741	48.4	0.0	-80.0	-1.2	0.027	-1.8	0.0
47810.850	0.674	29.0	0.1	-48.5	0.1	0.171	2.2	0.0
47812.871	0.150	-73.8	-1.4	109.2	0.4	0.172	0.7	-1.4
47813.898	0.393	-37.8	-0.2	55.8	0.4	0.173	1.8	-0.2
47814.887	0.626	15.8	-0.2	-29.8	-1.4	0.173	1.8	-0.2
47917.762	0.882	89.4	-0.5	—	—	0.231	-0.4	-0.6

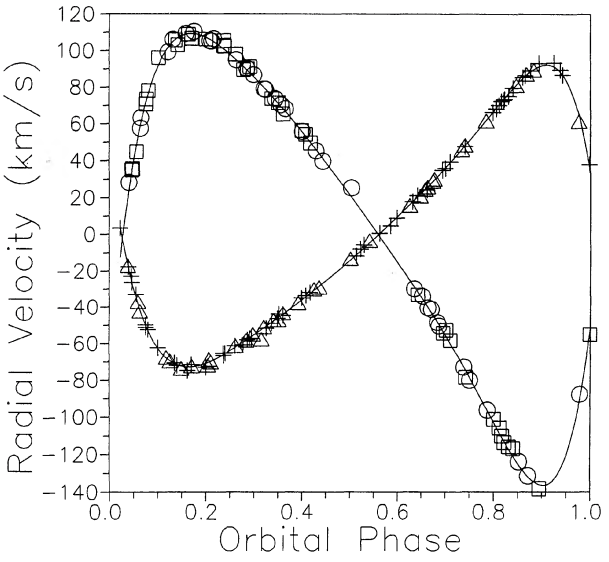

FIG. 4. Short-period radial-velocity curves for *Ba* and *Bb*. The crosses indicate photographic plate measurements of *Ba* and the triangles show Reticon or CCD observations of *Ba*. The squares symbolize photographic plate measurements of *Bb*, while Reticon or CCD observations are represented by the circles. The solid curves represent the short-period elements of Table 5.

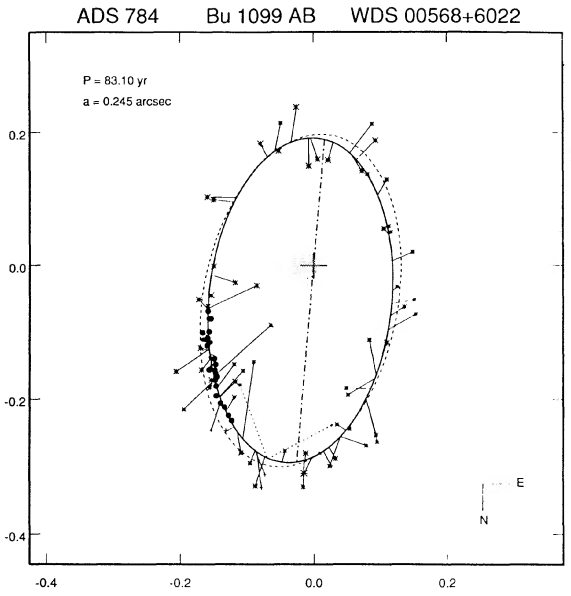

FIG. 6. Visual orbit of the long-period system Bu 1099 AB. Visual observations are indicated by plus signs or asterisks (for "small" or "large" telescope apertures, respectively—see Hartkopf *et al.* 1989), scaled in size according to their relative weight in the orbit solution. CHARA speckle observations are shown as filled circles, while other speckle observations are indicated by open circles. The shaded region represents the separation regime within 30 mas, the limit of resolution for a 4 m telescope. The line of nodes and O — C lines are also shown; points given zero weight in the orbit solution are indicated by dotted O — C lines. Finally, the dotted orbit is that of Heintz (1978a). Axes are in seconds of arc.

Although the speckle data were insufficient to derive all seven visual elements, the combination of spectroscopic and speckle data have yielded a complete preliminary description of the intermediate-period orbit, using the following method:

(1) The speckle data were averaged to give "normal points," reducing the scatter in the observations.

(2) The four elements derived spectroscopically (P_I, T_I, e_I, and ω_I) were adopted.

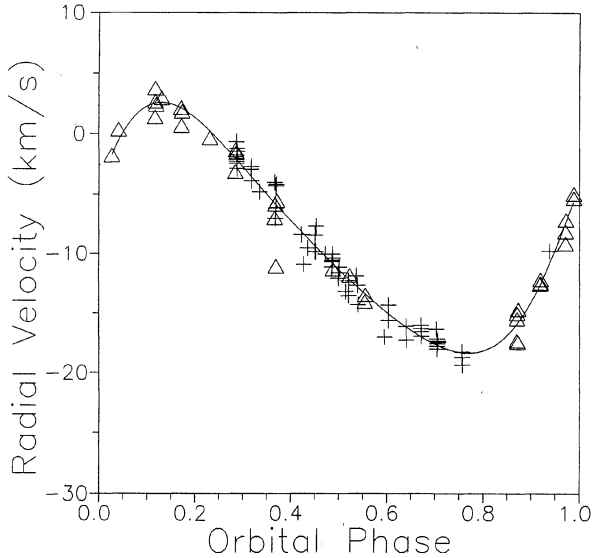

FIG. 5. Intermediate-period radial-velocity curve for *Ba*. The crosses indicate photographic plate measurements of *Ba*, while the triangles show Reticon or CCD observations of *Ba*. The solid curve represents the intermediate-period elements of Table 5.

(3) The remaining three elements (a_I'', i_I, and Ω_I) were determined by a grid search (Hartkopf *et al.* 1989) calculating rms residual errors at increments of 5° in i_I and Ω_I and 0".0005 in a_I'' (over the range 2–8 marcsec). Similar grid searches were carried out with various weighting schemes and also with all points rather than normal points; similar results were found by nearly all methods. Due to the marginal speckle detection of this component, an "eyeball estimate" was used in determining the final best fit. A particularly interesting result is that the "best-estimate" values of the inclination fell in the range 50° to 60°. Since the 83 yr period and 4.2 d period orbits appear to have similar inclinations near 55°; it now seems that all three orbits may be coplanar.

Resulting elements are listed in Table 5, with their estimated errors; Table 7 gives residuals to the speckle observations for both the long-period and the combined intermediate- and long-period orbit. A plot of that portion of the long-period orbit covered by speckle observations is shown in Fig. 7, together with the best fit combined intermediate- and long-period orbit and the speckle normal points used in the fit.

5. DISCUSSION

The elements of the various orbits listed in Table 5 have been used to determine some of the other physical parameters of HR 266.

The system as a whole was classified as B9 V by Cowley *et*

TABLE 7. Residuals to the long- and intermediate-period visual orbits.

Date	Code	Wt	θ_o (deg)	ρ_o (″)	θ_L (deg)	ρ_L (″)	$\Delta\theta_L$ (deg)	$\Delta\rho_L$ (mas)	ΔX_L (mas)	ΔY_L (mas)	θ_{LI} (deg)	ρ_{LI} (″)	$\Delta\theta_{LI}$ (deg)	$\Delta\rho_{LI}$ (mas)	ΔX_{LI} (mas)	ΔY_{LI} (mas)
1977.6353	A6	10	293.9	0.174	291.3	0.170	2.7	4	-1	9	292.5	0.173	1.5	1	1	5
1977.7333	A5	20	293.4	0.173	291.8	0.171	1.7	2	0	5	293.0	0.173	0.5	-0	1	1
1978.5414	A5	20	297.0	0.176	295.7	0.176	1.4	-0	2	4	296.8	0.177	0.3	-1	1	1
1978.6100	A5	20	297.4	0.174	296.0	0.177	1.5	-3	5	3	297.0	0.177	0.5	-3	3	0
1978.6154	A5	20	297.2	0.175	296.0	0.177	1.2	-2	3	3	297.0	0.177	0.2	-2	2	-0
1979.7703	A7	20	302.3	0.186	301.1	0.186	1.2	1	2	4	300.3	0.184	2.1	2	2	7
1980.4854	A8	20	301.1	0.195	304.1	0.191	-2.9	4	-9	-6	303.1	0.191	-1.9	4	-7	-3
1980.7178	A8	20	304.4	0.193	305.0	0.193	-0.5	0	-1	-1	304.1	0.194	0.4	-1	1	1
1980.7233	A8	20	304.5	0.196	305.0	0.193	-0.5	3	-3	1	304.1	0.194	0.4	2	-1	3
1980.8817	A10	10	306.6	0.193	305.6	0.194	1.0	-1	3	2	304.9	0.196	1.8	-3	6	4
1980.8925	A10	10	303.7	0.200	305.7	0.194	-1.9	6	-9	-2	304.9	0.196	-1.2	4	-6	-1
1981.7036	A9	20	306.9	0.200	308.7	0.201	-1.7	-1	-3	-5	308.7	0.204	-1.7	-4	-1	-7
1982.5088	C2	20	315.1	0.209	311.5	0.207	3.7	2	8	11	312.2	0.211	3.0	-2	9	7
1982.6030	R8	5	311.8	0.206	311.8	0.208	0.0	-2	2	-1	312.5	0.211	-0.7	-5	2	-5
1982.7601	C2	20	313.0	0.205	312.3	0.209	0.7	-5	5	-1	313.1	0.212	-0.1	-8	5	-5
1983.0690	C2	20	314.7	0.222	313.4	0.212	1.4	10	-3	11	314.2	0.214	0.6	8	-4	7
1983.9547	R11	5	314.8	0.220	316.1	0.219	-1.3	1	-4	-3	316.4	0.217	-1.6	3	-6	-2
1984.0547	C2	20	316.5	0.216	316.4	0.220	0.1	-3	3	-2	316.6	0.218	-0.1	-2	1	-1
1984.7015	C2	20	318.3	0.220	318.3	0.225	0.0	-4	3	-3	317.7	0.222	0.7	-2	3	0
1984.7860	R12	5	318.9	0.224	318.6	0.225	0.4	-1	2	0	317.9	0.223	1.1	1	3	4
1984.9965	C2	20	319.1	0.226	319.2	0.227	-0.1	-1	0	-1	318.4	0.225	0.7	1	1	3
1984.9993	C2	20	318.7	0.221	319.2	0.227	-0.5	-6	3	-6	318.4	0.225	0.3	-5	4	-3
1985.7520	R16	0	319.1	0.220	321.2	0.233	-2.1	-13	2	-15	320.5	0.234	-1.4	-14	5	-14
1985.8402	C2	20	320.8	0.232	321.5	0.234	-0.7	-1	-1	-3	320.8	0.235	0.0	-2	1	-2
1986.8860	C4	20	323.0	0.244	324.2	0.241	-1.1	3	-5	-1	324.2	0.245	-1.2	-1	-3	-4
1987.7570	C4	20	325.8	0.249	326.3	0.248	-0.5	1	-2	-0	326.9	0.251	-1.1	-2	-3	-4
1988.6553	C5	20	327.5	0.251	328.4	0.254	-0.8	-3	-1	-5	328.8	0.253	-1.2	-3	-3	-5
1989.7064	C6	20	330.2	0.258	330.7	0.261	-0.5	-3	-1	-3	330.1	0.258	0.1	0	0	0
1990.7549	C6	20	331.9	0.262	332.9	0.267	-0.9	-5	-2	-6	332.3	0.268	-0.4	-5	1	-5
rms residuals:									3.7	4.8					3.4	4.0

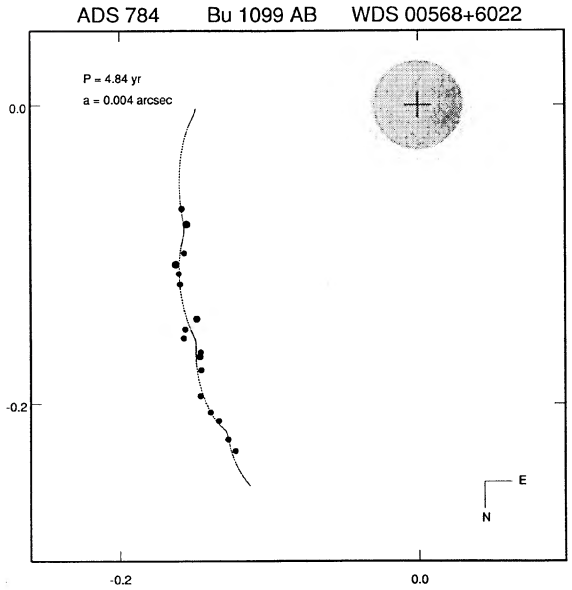

FIG. 7. A portion of the long-period orbit, perturbed by the 5 yr astrometric orbit. Speckle "normal" points are indicated by filled circles. P_I, T_I, e_I, and ω_I for the intermediate-period orbit were adopted from the spectroscopic solution. Thus, the period, phase, and general shape of the perturbation are fixed. Axes are in seconds of arc.

al. (1969) and as B9 IV by Abt (1981). The Stromgren photometry of Crawford *et al.* (1973) and Hβ photometry of Crawford (1963), according to Crawford's (1978) spectral type calibration for late B stars, are consistent with all components being dwarfs. However, there is not enough difference in β or c_0 between luminosity class V and III stars to rule out the possibility that at least one of the stars is a subgiant. Thus, several possible scenarios are examined, assuming various spectral types and masses for *Ba* and *Bb*.

First, if a mass of 2.6$\mathcal{M}_\odot$ (Popper 1980) is assumed from the B9 V classification of *Ba*, the resulting mass of *Bb* would be 1.7$\mathcal{M}_\odot$. This implies a late A star (Popper 1980). Is this consistent with the magnitude difference of the components?

The relative line intensities of Mg II 4481 Å and several Fe II lines near 4500 Å for *Ba* and *Bb* were measured in several CCD spectra. A magnitude difference of 0.5 mag was calculated from the Fe II line intensities. However, Wright *et al.* (1963) show that these lines increase rapidly in strength from A0 to A2, so this line ratio is not a good indicator of the magnitude difference of the close pair. The strength of the Mg II line, which appears to be a better indicator (Wright *et al.* 1963), results in a magnitude difference of 1.3 mag. From the spectral type—absolute magnitude relation of Corbally & Garrison (1984), the V magnitude difference between a B9 V star and a late A dwarf is about 2.2 mag. This magnitude difference is significantly larger than the one calculated from the line intensities. With a magnitude difference this

large, it is unlikely that the lines of the fainter star, *Bb*, would be seen, particularly in the photographic spectrograms. The derived masses and magnitude differences lead to inconsistencies if *Ba* and *Bb* are both dwarfs.

An alternative model of the system is that *Ba* is a significantly evolved main-sequence star or subgiant, which we will classify as a B9 IV star, and that the classification of *Bb* as A1 V is correct. The assumed mass of *Bb*, 2.25 ± 0.16 $\mathcal{M}_\odot$, was found by averaging the masses of eight stars of similar spectral type listed in Popper (1980), Lacy (1982), Andersen *et al.* (1984), Andersen & Gimenez (1985), and Tomkin & Popper (1986). Assuming such a mass, the mass of *Ba* is 3.4 ± 0.8 $\mathcal{M}_\odot$, suggesting that it has evolved off the main sequence.

Corbally & Garrison (1984) give a V magnitude difference of 1.5 mag between a B9 IV star and an A1 V star. Such stars would have a similar magnitude difference in B. This is more consistent with the magnitude difference estimated from the Mg II line than the previous model of the system. According to Corbally & Garrison (1984), the A component, which Fekel (1979) classified as B7 V, would still be 0.3 mag brighter than *Ba*. However, if it is more massive than the *Ba* component, it should also be a subgiant, increasing the magnitude difference. This model appears to be the more consistent one and will be assumed in the following discussion.

From the mass function of the intermediate-period orbit and the assumed masses of *Ba* and *Bb*, the mass of *Bc* was computed. A minimum value of 2.3 ± 0.4 $\mathcal{M}_\odot$ was found by setting $\sin i_I$ equal to 1. If this orbit is indeed coplanar with the long- and short-period orbits, then $\mathcal{M}_{Bc}$ would be 2.8 ± 0.8 $\mathcal{M}_\odot$.

The submotion in the speckle data can be regarded as the classical astrometric perturbation in which the observed photocentric motion is displaced from the barycenter toward the primary, in this case components *Bab*, by an amount dependent on the $\Delta m_{Bab,c}$ and on the fractional mass $\mathcal{M}_{Bc}/(\mathcal{M}_{Bab} + \mathcal{M}_{Bc})$ (van de Kamp 1967). Adopting $\Delta m_{Bab} = +1.3$ from the spectroscopic analysis and using reasonable values in a bolometric corrected mass-luminosity relation (Heintz 1978b), a *Bc* component of $2.8\mathcal{M}_\odot$ would be approximately 0.1 mag brighter than *Bb*, 1.2 mag fainter than *Ba*, and 2.2 mag fainter than *A*, the primary of the visual binary.

If *Bc* were a rapidly rotating and hence a broad-lined, single star, it would only contribute marginally to the spectrum—its broad spectral features dominated by the similarly broad but strong features of the A component. As seen from Fig. 1, the broad features of A, which underlie the sharp features from the B components, only represent a few percent of the continuum, and so whatever contribution is present from *Bc* must be at the 1% level or weaker.

These mass-luminosity considerations permit the estimation of the actual semimajor axis from the observed photocentric semimajor axis of 0".004. The rather large error associated with the mass of *Bc* can be used to find a range in likely true semimajor axes of 0".024 to 0".045. The corresponding values of $\Delta m_{Bab,c}$ over this same range are $+2.0$ to $+0.9$ in the sense that the larger semimajor axis is associated with the smaller magnitude difference. The fact that there is no indication in any of the speckle observations that the *Bab,c* system is resolved implies that the favorable case of large semimajor axis and smaller magnitude difference is not present. Speckle or other interferometric observations with larger apertures (or longer baselines) than 4 m may place further constraints on this intermediate period system or may even resolve the *Bab,c* orbit directly.

Another possibility is that the *Bc* component is actually a close pair of stars of later spectral type, making the mass of *Bc* the sum of the two components' masses. This would explain *Bc* having a large mass but no detectable absorption lines in the spectra. If this is the case, HR 266 would be a quintuple system.

With a mass of $2.25\mathcal{M}_\odot$ for *Bb* and the minimum mass from Table 5, i_S is $54°.2 \pm 4°.9$. This range for the inclination of the short-period orbit includes the values of the inclination of the long-period or visual orbit found by Heintz (1978a) and the intermediate- and long-period orbits of this paper, indicating that all three orbits may be coplanar.

If component A is a B7 IV star, we estimate a mass of about $5\mathcal{M}_\odot$. For coplanar orbits the total mass of the system becomes $13.4\mathcal{M}_\odot$. From Kepler's third law and P_L and a_L (Table 5), the geometric parallax of the system is 0".0054 for a distance of 185 pc. The parallax can also be estimated from the assumed absolute visual magnitudes taken from Table 1 of Corbally & Garrison (1984). These magnitudes result in a parallax of 0".0038. If all stars are assumed to be main-sequence stars, the parallax increases to 0".0045. Since the parallax depends only on the cube root of the assumed masses, the geometric parallax is probably more accurate than the parallax determined from the magnitudes. The derived properties of the system are summarized in Table 8.

Other quantities indicate further properties of HR 266. The mass ratio of the *Bc* component to the short-period binary, $\mathcal{M}_{Bc}/\mathcal{M}_{Bab}$, is 0.5. According to Fekel (1981), 72% of the triple systems he considered had mass ratios between 0.4 and 0.67. Thus, the spectroscopic triple system appears to have a fairly typical mass ratio. The period ratios have the values: $P_I/P_S = 417$ and $P_L/P_I = 17.2$. These appear consistent with the finding of Fekel (1981) that more massive stars have smaller period ratios. From Bodenheimer's (1978) model, HR 266 should have a large ratio of spin to angular momentum since its period ratio is small. Such a conclusion is supported by the presence of the rapidly rotating A component, for which we measured a $v \sin i$ of 270 ± 15 km s^{-1}. For both *Ba* and *Bb* $v \sin i$ is $\leqslant 5$ km s^{-1}. As stated previously, the system is probably coplanar. This would rank it among the two thirds of the systems studied by Fekel (1981) that might be coplanar.

A survey of the Eighth Catalogue of the Orbital Elements of Spectroscopic Binary Systems (Batten *et al.* 1989) was made to determine if the large eccentricity of the short-period pair is unusual. From the list, 241 or about 16% of the systems were found to have periods less than 10.0 d and e greater than or equal to 0.05. Twenty-four (1.6%) of these

TABLE 8. Assumed properties of HR 266 = ADS 784.

Component	Spectral type	M_V	Mass ($\mathcal{M}_\odot$)	$v \sin i$ (km s^{-1})
A	B7 IV	−1.0	5.0	270
Ba	B9 IV	−0.3	3.4	⩽5
Bb	A1 V	1.2	2.25	⩽5
Bc			2.8	
Parallax		0".0038	0".0054	
Distance		263 pc	185 pc	

binaries had eccentricities greater than 0.4 but only eight of these also had periods less than 5 d and four of the eight were graded as *e* quality or unreliable orbits. There appears to be at least one other binary, HD 24769, with a similar spectral type (B9.5 IV), a short period (1.59 d), and a high eccentricity (0.37). Although the large eccentricity of the *Bab* pair is quite unusual, HR 266 does not appear to be unique.

Can the short-period binary really consist of an evolved subgiant component and still have such a large eccentricity? A theoretical circularization timescale was calculated with the theory of Tassoul (1988). A value of 2.7×10^8 yr was found, assuming $N=0$, $r_g=0.1$, $\mathscr{M}=3.4\mathscr{M}_\odot$, $R=2.23\,R_\odot$, $L=72.4\,L_\odot$. This was compared with the evolutionary theory for the age of the system. From the models of Maeder & Meynet (1988) the age of the system is found to be around 3.6×10^8 yr, larger than the estimated circularization timescale. However, due to the uncertainties of the mass of *Ba*, the possibility of it being a subgiant cannot be dismissed.

In conclusion, although our knowledge of HR 266 = ADS 784 is much improved, the complications posed by the presence of at least four stars is considerable. The attempt to determine the individual properties of the stars must be considered preliminary at best. The evolutionary state of the components needs confirmation and the nature of the unseen *Bc* component remains a mystery. An accurate magnitude difference for the visual pair would be very useful to further constrain the model. As noted previously, future speckle observations with larger aperture telescopes or longer baselines may resolve the stars of the intermediate-period orbit directly.

We thank Chris Aikman for obtaining and measuring several of the DAO plates. We are grateful for the assistance of Charles Worley in obtaining visual data from the Washington Visual Double Star Catalog, maintained by Worley at the U.S. Naval Observatory. The spectroscopic research was supported in part by NSF Grant No. AST 81-16409 and a grant from the Vanderbilt University Research Council (F.C.F.). The speckle program at Georgia State University was supported by NSF grants during the course of data acquisition and most recently by NSF Grant No. AST 89-15324.

REFERENCES

Abt, H. A., Sanwal, N. B., & Levy, S. G. 1980, ApJS, 43, 549
Abt, H. A. 1981, ApJS, 45, 437
Al-Shukri, A. 1991, Ph.D. thesis, Georgia State University
Andersen, J., Clausen, J. V., & Nordström, B. 1984, A&A, 134, 147
Andersen, J., & Gimenez, A. 1985, A&A, 145, 206
Barker, E. S., Evans, D. S., & Laing, J. D. 1967, R. Obs. Bull., 130
Batten, A. H., Fletcher, J. M., & MacCarthy, D. G. 1989, Publ. DAO, 17,1
Bodenheimer, P. 1978, ApJ, 224, 488
Bopp, B. W., Evans, D. S., & Laing, J. D. 1970, MNRAS, 147, 355 (with an Appendix by T. J. Deeming)
Burnham, S. W. 1906, A Catalogue of Double Stars, Part II (Carnegie Institution of Washington, Washington, DC), p. 286
Campbell, W. W., & Moore, J. H. 1928, Publ. Lick Obs., 16, 272
Corbally, C. J., & Garrison, R. F. 1984, The MK Process and Stellar Classification, edited by R. F. Garrison (David Dunlap Observatory, Toronto), p. 277
Cowley, A., Cowley, C., Jaschek, M., & Jaschek, C. 1969, AJ, 74, 375
Crawford, D. L. 1963, ApJ, 137, 530
Crawford, D. L., Barnes, J. V., Golson, J. C., & Hube, D. P. 1973, AJ, 78, 738
Crawford, D. L. 1978, AJ, 83, 48
Daniels, Jr., W. 1966, University of Maryland, Dept. of Physics & Astronomy Technical Report No. 579
Evans, D. C. 1968, MNRAS, 141, 109
Fekel, F. C. 1992, unpublished
Fekel, F. C. 1979, Ph.D. thesis, University of Texas
Fekel, F. C. 1981, ApJ, 246, 879
Fekel, F. C. 1985, in Stellar Radial Velocities, IAU Colloquium No. 88, edited by G. D. Philip and D. Latham (Davis, Schenectady), p. 335
Fekel, F. C., Bopp, B. W., & Lacy, C. H. 1978, AJ, 83, 1445
Frost, E. B., Barrett, S. B., & Struve, O. 1926, ApJ, 64, 1
Hartkopf, W. I., McAlister, H. A., & Franz, O. G. 1989, AJ, 98, 1014
Heintz, W. D. 1978a, ApJS, 37, 71
Heintz, W. D. 1978b, Double Stars (Reidel, Dordrecht), p. 60
Lacy, C. H. 1982, ApJ, 261, 612
Maeder, A., & Meynet G. 1988, A&AS, 76, 411
McAlister, H. A., & Hartkopf, W. I. 1988 Second Catalog of Interferometric Measurements of Binary Stars, CHARA Contribution No. 2
McAlister, H. A., Hartkopf, W. I., & Franz, O. G. 1990, AJ, 99, 965
Morgan, W. W. 1931, ApJ, 73, 104
Palmer, E. R. Walker, E. N., Jones, D. H. P., & Wallis, R. E. 1968, R. Obs. Bull., 135
Pearce, J. A. 1957, Trans. IAU, 9, 441
Petrie, R. M., & Batten, A. H., 1970, Publ. DAO, 13, 383
Plaskett, J. S., Harper, W. E., Young, R. K., & Plaskett, H. H. 1922, Publ. DAO, 1, 287
Popper, D. M. 1980, ARA&A, 18, 115
Scarfe, C. D., Batten, A. H., & Fletcher, J. M. 1990, Publ. DAO, 18, 21
Stickland, D. J. 1980, private communication
Stickland, D. J., & Weatherby, J. 1984, A&AS, 57, 55
Tassoul, J. 1988, ApJ, 324, L71
Tomkin, J., & Popper, D. M. 1986, AJ, 91, 1428
van de Kamp, P. 1967, Principles of Astrometry (Freeman, San Francisco), p. 167
Vogt, S. S., Tull, R. G., & Kelton P. 1978, Appl. Opt., 17, 574
Worley, C. E. 1990, Washington Visual Double Star Catalogue (computer master catalogue maintained by Worley at the U.S. Naval Observatory, Washington, DC)
Wolfe, Jr., R. H., Horak, H. G., & Storer, N. W. 1967, Modern Astrophysics, edited by M. Hack (Gordon and Breach, New York), p. 251
Wright, K. O., Lee, E. K., Jacobson, T. V., & Greenstein, J. L. 1963, Publ. DAO, 12, 173